CONF-8811161--1

DE89 006685

X-RAY DIFFRACTION FROM ION IMPLANTED ZONES

Satish I. Rao, Charles R. Houska, Department of Materials Engineering, Virginia Polytechnic Institute and State University, Blacksburg, Virginia 24061; K. Grabowski and J. Claussen, Naval Research Laboratory, Washington, D.C., 20375; and G. Ice and A. Habenschuss, X-14 NSLS, Brookhaven National Laboratory, Upton, NY 11973.

ABSTRACT

Measurements of x-ray profiles and diffuse scattering from (111), (100) single crystal Niobium films implanted with Nitrogen to average levels of 5 and 0.5 atomic percent are discussed. Theoretical analysis of the asymmetric profiles are used to determine the strain profile in the implanted films. The measured strain profile results from two factors: (i) depth distribution of implants and knock-on damage and (ii) elastic constraints. Residual elastic strains develop due to the constraints imposed by a sapphire substrate. Comparison of the diffraction results with theoretical predictions of TRIM indicates the presence of measurable knock-on damage in the films. Huang and Stokes-Wilson scattering measurements made using synchrotron radiation at the ORNL beamline, Brookhaven National Laboratory, were used to reveal the identity of defects formed during the knock-on process.

INTRODUCTION

Primary solutions are under examination containing single foreign interstitials which remain unclustered in octahedral sites [1] because of the choice of low implantation temperatures. An energetic interstitial atom produces damage related self interstitials, and vacancies. Self interstitials and vacancies produced by damage become segregated, due to enhanced diffusion, into a distribution of small loops at liquid nitrogen temperature.

Four implantation energies were used to produce four overlapping Gaussian distributions of N in a 2500A Nb single crystal film deposited onto a thick (001) sapphire crystal. This gives a nonuniform concentration when superimposed giving an average of 5 at % N. Variations about the average composition produce related variations in the interplanar spacing. Bragg peaks become broadened into intensity bands with a characteristic fine structure which is used to obtain the distribution of interplanar spacing below the free surface. Diffraction theory was developed to allow for the rather large effect of static displacement fields about interstitial implants as well as damage related defects. Kinematic theory was used throughout these developments because of the relatively large distortions encountered in high fluence ion-implantation problems.

We find that the distribution of interplanar spacings is 15% larger than that predicted theoretically by TRIM. This has been shown to be related to the excess expansion from residual

The submitted manuscript has been authored by a contractor of the U.S. Government under contract No. DE-AC05-84OR21400. Accordingly, the U.S. Government retains a nonexclusive, royalty-free license to publish or reproduce the published form of this contribution, or allow others to do so, for U.S. Government purposes.

MASTER

DISTRIBUTION OF THIS DOCUMENT IS UNLIMITED

knock-on damage. Both implanted N and knock-on defect arrangements can produce a lattice expansion and related compressive stresses. Although some stress relaxation results from field cancellation between interstitial and vacancy loops, complete cancellation does not occur for small loops due to core effects.

ELASTIC-FREE EXPANSION STRAINS

Consider the overall implanted zone to be contained within semi rigid walls and that it responds elastically without relaxations associated with plastic deformation. That is, the underlying material does not allow a free expansion of the zone. The strains (and stresses) that develop along the implanted zone can be calculated using the method of strain suppression [2].

In treating the purely elastic problem, the implanted zone is allowed to expand freely as uncoupled slabs of constant concentration "C_i" and a thickness dx_3. Each slab undergoes a free expansion (or contraction) due to the pressure exerted by the implanted atoms and knock-on defects. We know that a concentration "C_i" of one kind of point defect and orientation produces a bulk expansion of the lattice given by [3].

$$\sum_{i=1}^{3} \epsilon_{ii} = \frac{C_i}{V} \frac{\partial V}{\partial C_i} \tag{1}$$

where ϵ_{ii} are the diagonal components of the strain tensor, expressed in terms of the cubic coordinate system. Cubic symmetry is maintained by allowing each of the axes of the principal strain to be oriented along mutually perpendicular directions in equal numbers. Isotropy is normally lost when the slabs are joined continuously [4] by the method of strain suppression. The elastic strain profile, expressed in terms of the sample coordinate system, is directly proportional to the variation of "$\dot{C}$". Slabs are joined together continuously making the total strain along the 1′ and 2′ parallel to the free surface, essentially zero throughout the implanted zone.

The normal elastic strain, at an angle χ to the x_3 direction, is obtained from [4].

$$\epsilon'_{e\chi}(x_3) = \{ \epsilon'_{e11}(x_3) - \epsilon'_{e33}(x_3)\}\sin^2\chi + \epsilon'_{e33}(x_3) \tag{2}$$

or

$$\epsilon'_{e\chi}(x_3) = \frac{C(x_3)}{3V} \frac{\partial V}{\partial C} \{ -\beta^{el}\sin^2\chi - A\} \tag{3}$$

where

$$\beta^{el} = \frac{C_{11} + 2C_{12}}{C_{11} + C_{an}\Omega} = 1 - A \tag{4}$$

and Ω relates to the transformation to the sample coordinate system [4]. The total strain in the implanted zone, at tilt angle χ, includes the free expansion strain and the elastic strain, i.e.

$$\epsilon_{\chi}'(x_3) = \frac{C(x_3')}{3V} \frac{\partial V}{\partial C} \beta^{el} \cos^2\chi \qquad (5)$$

The measured strain goes to zero linearly with a $\cos^2\chi$ dependence, at $\chi = 90°$. The ratio of the total strain at $\chi = 0°$, to the free expansion strain is β^{el} which is a magnification factor that can be as large as 2-3. At an angle $\chi = \chi_o$, the total strain is identically equal to the free expansion i.e.

$$\cos^2\chi_0 = 1 / \beta^{el} \text{ or } \sin^2\chi_0 = - A / \beta^{el} \qquad (6)$$

The main features of the strain equations are illustrated in Fig. 1 for one element.

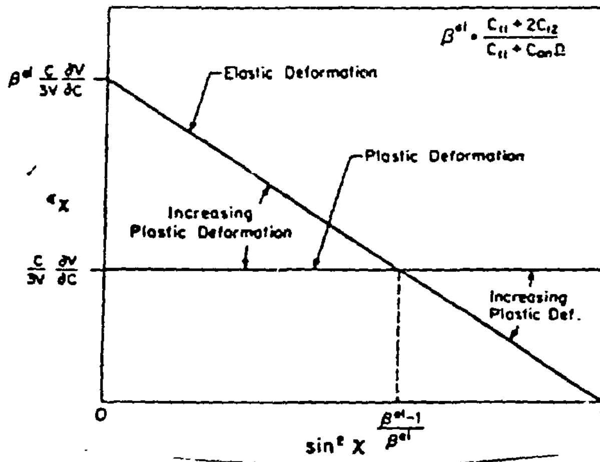

FIG. 1. Plots of Eq. (6) with and without β^{el} expansion factor i.e completely elastic or completely relaxed by plastic deformation ($\beta^{el} = 1$).

A measurement of the strain profile at various tilt angles χ, allows one to separate the free expansion gradient from the elastic strain gradient. X-ray intensity band analysis is used to determine the strain profile and is discussed in a later paper.

If the concentrations are sufficiently small, these results can be applied to more than one type of defect by summing over all defect species, "j" to obtain the free expansion profile. The profile obtained when the sample is elastically constrained is obtained by simply multiplying by β^{el}.

INTENSITY DISTRIBUTION FROM ELASTICALLY CONSTRAINED ZONE

If the implanted zone is completely constrained by the underlying substrate, then the displacement components along a_1 and a_2 directions, X_m and Y_m, are identically equal to zero. Therefore, the strains ϵ_{33}', is only a function of x_3. By introducing these simplifications, and summing over each layer, one obtains

$$I = K'F^2 \frac{\sin^2\pi N_1 h_1'}{(\pi N_1 h_1')^2} \frac{\sin^2\pi N_2 h_2'}{(\pi N_2 h_2')^2} \sum_{m_3} \sum_{m_3'} e^{-M(m_3)} e^{-M(m_3')} e^{2\pi i \ell (Z_{m3}' - Z_{m3}')} e^{2\pi i (m_3 - m_3') h_3} \qquad (7)$$

where K' is constant over one intensity band, F is the structure factor for the normal unit cell. $N_1 a_1$ and $N_2 a_2$ are the dimensions of the crystal along a_1 and a_2 directions parallel to the free

surface and $h_1' = (h_1 - h)$, $h_2' = (h_2 - k)$ are variables in reciprocal space. The exponentials containing $M(m_3)$ and $M(m_3')$ are static attenuation factors determined by the implants and loops [1,5]. If N_1a_1 and N_2a_2 are taken to be large, the intensity in reciprocal space is spread only along the h_3 direction, and is a product of delta functions with respect to the h_1' and h_2' dependence. The variation of the intensity along the h_3 direction is obtained by numerically summing Eq. (7) over the entire implanted zone.

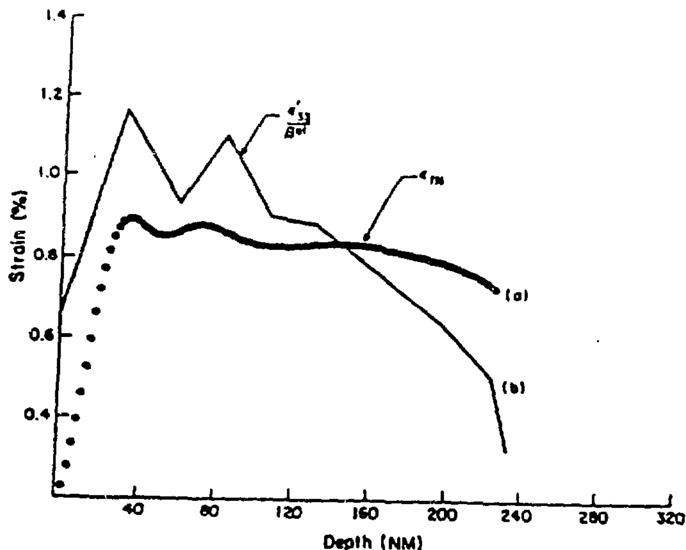

FIG. 2. Free expansion strain profiles for multiply implanted N into a 2500A (111) oriented Nb film on (001) sapphire. Determined from (a) TRIM simulations (b) x-ray intensity band analysis.

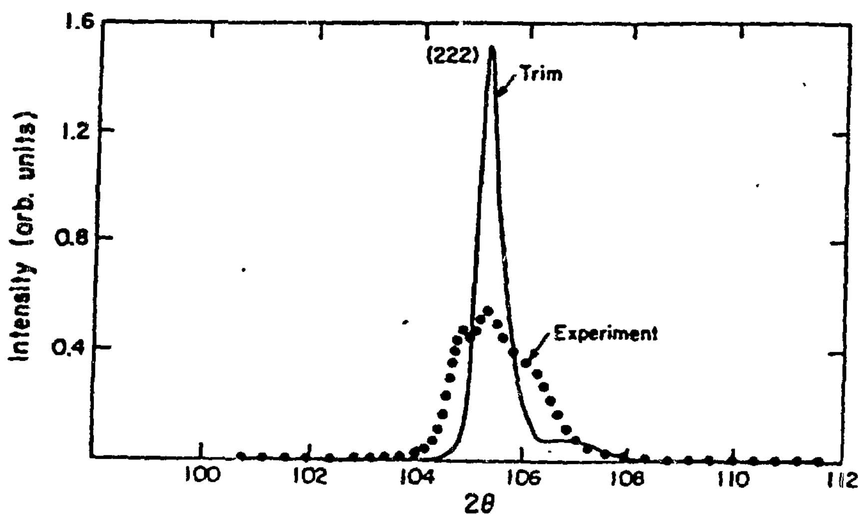

FIG. 3.

(222) intensity band from TRIM obtained with curve in Fig. 2(a) using Eq. (7).

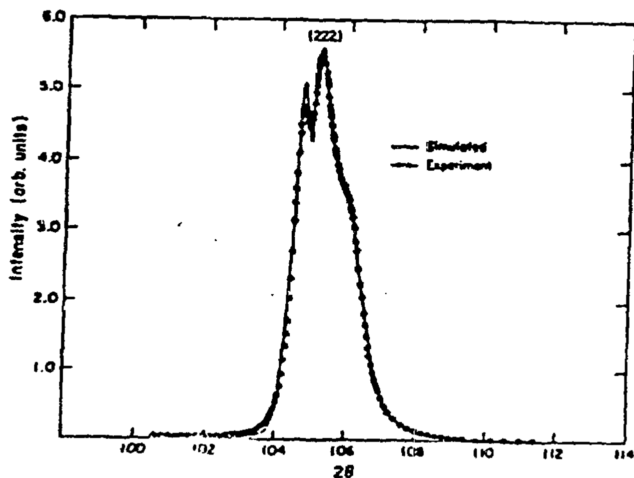

FIG. 4. Experimental (222) intensity band compared with the intensity profile obtained with the curve in Fig. 2(b) using Eq. (7).

Figure 2(b) shows an experimentally determined strain profile along the multiply implanted Nb film and the division of such a zone into connecting linear regions. The assumption of linear gradients introduces sawtooth regions in the strain profile when the strain gradient changes sign. A sinusoidal representation of the strain profile would eliminate the sawtooth discontinuities. However, under the present conditions, the end results from either analysis are not significantly altered.

Figure 3 illustrates the (222) intensity band from strain profile Fig. 2a obtained from TRIM calculations. Clearly, this does not fit. Also, TRIM calculations do not account for the Nb sapphire interface. Figure 4 illustrates our best fit to the experimental intensity band and gives the experimental curve in Fig. 2(a). The x-ray analysis shows a strain profile that contains additional detail near the surface and appears to go to zero near the interface. The TRIM calculation should not be considered beyond 160 nm. However, the peak location is in agreement with the constrained elastic model.

A preliminary examination of a (100) Nb film implanted under the same conditions as the (111) orientation gives an intensity band which differs from the results shown with a (111) film. However, the results indicate that they are in accord with an elastically contrained model.

The (222) planes are parallel to the free surface so that the data are obtained from a radial scan. If this is transformed to (001), bands of the type $hk\ell$ must be projected. At an angle of inclination χ corresponding to the ($hk\ell$) band, the projection is given by

$$\cos\chi = \frac{\ell}{\sqrt{h^2 + k^2 + \ell^2}} \tag{8}$$

When this holds, the spread of the intensity along an ($hk\ell$) band in the "h_3" direction is identical to the distribution around the corresponding (00ℓ) point. A detailed study of six intensity bands was used to determine the strain distribution along the implanted zone and assess whether the strains along the 1′, 2′ directions are zero.

If particle size broadening is negligible, one can show that the strain broadening is proportional to ℓ [6] and one can inter-relate ($hk\ell$) distributions to the (001) distribution. The spread in radians is proportional to the overall strain and described by

$$\Delta 2\theta(\text{rad}) = 2(\,\varepsilon \cos^2\chi)\tan\theta \tag{9}$$

This gives the usual $\tan\theta$ relation between a shift in d-spacing and the related angular change. The additional $\cos^2\chi$ allows for the projection along an angle χ. If this dependence is obeyed, then the purely elastic model is verified and particle size broadening is negligible. These data are examined in detail in a later paper.

LATTICE DAMAGE

A (111) Nb film was implanted to an average composition of 0.5% N at LNT to reduce the d-spacing broadening and thereby allow diffuse scattering data to be collected. We have charac-

terized the knock-on defect structures with Huang-Stokes-Wilson x-ray diffuse scattering using Larson plots [7]. This required a difference to be taken between the data from implanted and unimplanted single crystal Nb films. Statistically meaningful data could only be obtained with synchrotron radiation. This diffuse scattering, resulting from long range elastic displacement fields, and can be explained by vacancy and self interstitial loops of like size distributions with radii extending from 5-15A.

The displacement field from knock-on damage has been identified as loops on (211) planes using an anisotropic calculation by Ohr [8]. Self interstitial and vacancy loops have like displacement fields except for a change in sign i.e interstitial loops give a positive displacement along the loop axis while vacancy loops give negative values. Although this cancels some of the displacement field, the cores continue to make a contribution and account for the 15% difference between the x-ray results and TRIM in the range from 0 to 140 nm (Fig 2).

At 0.5% N, most of the expansion is due to lattice damage and this is close to the level found at 5%. Someplace in between these concentrations, the lattice damage appears to saturate causing the lattice disturbance from an increasing number of interstitial N defects to dominate.

Simulations using expanded versions of TRIM are capable of giving the distribution of energy loss due to knock-on collisions. We were encouraged to find that this follows the same general form as the excess in d-spacing which is attributed to residual knock-on damage.

CONCLUSIONS

1. For a 5 at % implantation of N in Nb at LNT, the dominant elastic strain is due to single N interstitials.

2. At a lower level of (0.50 at % N) knock-on lattice damage is sufficiently large and different relative to single interstitials to be measureable using Huang-Stokes-Wilson diffuse scattering from a single crystal film.

3. X-ray intensity band analysis provides a means of determining the strain profile along an implanted zone.

4. The strains remain elastic without observable plastic deformation.

ACKNOWLEDGEMENTS

We would like to acknowledge Professor D. Farkas for providing simulations of the energy deposition curves and the Office of Naval Research for sponsoring this research on Grant # N0004-83-K-0750, P00004. Research was performed in part at the Oak Ridge National Laboratory Beamline X-14 at the National Synchrotron Light Source, Brookhaven National Labora-

tory, sponsored by the Division of Materials Science and Division of Chemical Sciences, U.S. Department of Energy and under Contract DE-AC05-840R21400 with the Martin Marietta Energy Systems, Inc.

REFERENCES

1. S.I. Rao, E.J. Savino and C.R. Houska in 'Mat. Res. Soc. Symp. Proc.', V82, p187 (1987).
2. S. Timoshenko and J.N. Goodier, Theory of Elasticity (McGraw-Hill, N.Y., 1970).
3. P.H. Dederichs, J. Phys. F. 3, 471 (1973).
4. S.I. Rao and C.R. Houska, J. Appl. Phys. 52, 6322 (1981).
5. M.A. Krivoglaz, Theory of X-Ray and Thermal Neutron Scattering by Real Crystals (Plenum, New York, 1969).
6. C.R. Houska, J. Appl. Phys. 41, 69 (1970).
7. B.C. Larson and F.W. Young, Jr. in 'Point Defects and Defect Interaction in Metals' edited by Jin Ich Takamura, Masao Doyama and Michio Kiritani, University of Tokyo Press, p. 679 (1982).
8. S.M. Ohr, Phys. Stat. Sol. 64, 317 (1974).

DISCLAIMER

This report was prepared as an account of work sponsored by an agency of the United States Government. Neither the United States Government nor any agency thereof, nor any of their employees, makes any warranty, express or implied, or assumes any legal liability or responsibility for the accuracy, completeness, or usefulness of any information, apparatus, product, or process disclosed, or represents that its use would not infringe privately owned rights. Reference herein to any specific commercial product, process, or service by trade name, trademark, manufacturer, or otherwise does not necessarily constitute or imply its endorsement, recommendation, or favoring by the United States Government or any agency thereof. The views and opinions of authors expressed herein do not necessarily state or reflect those of the United States Government or any agency thereof.